P4.3 THE BEHAVIOR OF LOW-LEVEL VORTICITY AND CIRCULATION SURGES OF A MODELED SUPERCELL

Brian J. Gaudet and W.R. Cotton *
Dept. of Atmospheric Science, Colorado State University.

1. INTRODUCTION

There have been various numerical simulations that have examined the evolution of low-level vorticity in association with supercells (Klemp and Rotunno 1983; Grasso and Cotton 1985). Trajectory analyses have traditionally been used to quantify the vorticity evolution of the air parcels that compose the vorticity center (Rotunno and Klemp 1985; Wicker and Wilhelmson 1995; Adlerman et al. 1999). In such a backward trajectory analysis small errors in the computation of the velocity can rapidly propagate into large errors in position.

Here a Lagrangian (feature-fixed) method is used to investigate the behavior of an intense low-level vorticity center generated by a numerically-modeled supercell, but Eulerian (spatially-fixed) methods are also used to examine the vorticity and circulation budgets about this feature.

2. MODEL SETUP

The simulation was performed using the Regional Atmospheric Modeling System (RAMS) (Pielke et al. 1992). The model was initialized with an idealized supercell sounding used in Grasso (2000). The domain consisted of a single grid possessing 333 m grid spacing in the horizontal. The vertical grid spacing increased from a minimum of 40 m at the surface. A constant storm motion vector was subtracted from the velocities at the beginning of the simulation to allow the storm to stay on the grid. A warm moist bubble is used to initiate convection. The storm splits by 2700 s of simulation time, and the storms behave in a manner consistent with other modeled supercells in the literature. Also by 2700 s of simulation time mesocyclonic-strength (0.01 s^{-1}) vertical vorticity has formed along the main gust front of the right-mover. The rest of the analysis will focus on the right-mover during the time period from 2700 s until 3900 s.

3. VORTICITY BEHAVIOR

The location and value of the maximum vertical vorticity was found within the model domain at four separate levels: 19 m, 608 m, 234 m, and 1263 m above the surface. Figure 1 shows the grid-relative motion of the maximum vorticity at three of these levels, starting at 2700 s. At this time, mesocyclonic strength vorticity (0.016 s^{-1}) exists at the lowest model level along the gust front, with comparable vorticity values found aloft behind the surface gust front. However, starting at 3062 seconds, and continuing until 3222 s, the maximum vorticity values at all levels jump to a common location near the gust front triple point, beginning with the highest levels first. The vorticity maximum has a westward tilt of 1 km with height, but otherwise translates as a unit. Soon after this process, the vorticity intensifies by a factor of up to five near the surface, reaching 0.130 s^{-1} (Figure 2). The intensification appears to occur earliest and be more intense at the lowest levels, consistent with the findings of Grasso (1996) and Finley (1997) for their simulated vortices.

4. TENDENCY EQUATIONS

The inviscid Boussinesq vertical vorticity equation, in which incompressibility is assumed, and the Coriolis force as well as the direct production of vertical vorticity through solenoidal effects are neglected, is:

$$\frac{d\zeta_z}{dt} = (\zeta_{\mathbf{H}} \cdot \nabla)\mathbf{w} + \zeta_{\mathbf{z}} \frac{\partial \mathbf{w}}{\partial \mathbf{z}}, \quad (1)$$

where ζ_z is the vertical vorticity and ζ_H is the horizontal vorticity vector. The first term is referred to as the 'tilting term' whereas the second is the 'stretching term'. This equation is Lagrangian as it gives the vertical vorticity tendency following a trajectory.

The Eulerian version of this equation would provide the vertical vorticity tendency at a fixed point in space. It can be shown that this tendency can be written as the divergence of a flux (Haynes and McIntyre 1987; Weisman and Davis 1998):

$$\frac{\partial \zeta_z}{\partial t} = -\nabla \cdot (\mathbf{H} + \mathbf{V}), \quad (2)$$

where $\mathbf{H} = \zeta_z \mathbf{v_H}$ and $\mathbf{V} = w(\frac{\partial \mathbf{v_H}}{\partial \mathbf{z}} \times \hat{\mathbf{k}})$. The term $\mathbf{H}$ includes both horizontal advection and stretching, whereas $\mathbf{V}$ includes vertical advection and tilting.

The disadvantage of the Eulerian form is that the temporal history of vorticity following a trajectory is lost. However, the Eulerian equation closely corresponds to how vorticity evolves within the RAMS model, which computes advection using the divergence of momentum fluxes across the grid cell. Furthermore, the Eulerian equation can easily be integrated across several grid cells to give the circulation tendency around a spatially-fixed horizontal contour:

$$\frac{\partial C}{\partial t} = -\iint \nabla \cdot (\mathbf{H}+\mathbf{V}) dA = -\oint (\hat{\mathbf{k}} \times (\mathbf{H}+\mathbf{V})) \cdot \mathbf{dl}. \quad (3)$$

*Corresponding author address: Brian J. Gaudet, Dept. of Atmospheric Science, Colorado State University, Fort Collins, CO 80523; e-mail: gaudet@atmos.colostate.edu.

In this study the circulation and the circulation tendencies were examined using the line integral in 3 as applied to square horizontal contours at various heights in the model domain. The sizes of the curves were also varied. The smallest contour had a side of $1\Delta x$ and corresponded to a calculation of the discrete vorticity and Eulerian vorticity tendencies at a model grid point. Possible contour sizes included any square with a side that was an odd multiple of the grid spacing. All the contours were positioned so that the maximum model vorticity at the model height occurred in the center.

5. CIRCULATION BEHAVIOR

The motion of the vorticity centers suggest that their behavior is being forced from above. Grasso and Cotton (1995) and Wicker and Wilhelmson (1995) both suggested that dynamically-induced pressure deficits near cloud base induced convergence beneath them, which intensified the pre-existing vorticity beneath. In both cases strong, near-tornadic vortices developed.

For the idealized case of a Rankine vortex (an axisymmetric region with constant vorticity within a certain radius, and zero vorticity outside) in cyclostrophic wind balance, the pressure deficit of the vortex is proportional to the square of the circulation (Wicker and Wilhelmson 1995) and inversely proportional to the square of the radius of the vorticity center. Thus a vortex above the surface can cause a pressure minimum that initiates convergence and vortex stretching at progressively lower levels (Leslie 1971; Trapp and Davies-Jones 1997). In the present simulation, it was found that, whereas the maximum vorticity was located at the surface, the circulation around any contours larger than 1 km across was always at a minimum at the surface (Tables 1 and 2). Figure 3 shows that, for a square with dimension 3.7 km (eleven grid points per side), the circulation increases with height, but towards the time of maximum surface vorticity the circulation at all levels tends to converge to the value at 1263 m.

The circulation tendencies at the 1263 m level were examined. From Figure 4 it is clear that convergence of the horizontal vorticity flux is dominating the circulation evolution within approximately 3 km of the vortex. The term V only becomes positive at the highest level after the vortex has already intensified, due to vertical vorticity advection. Figure 5 shows the circulation tendencies at the lowest model level for the same distance from the vortex. As one might expect, the V term is insignificant at this height; the H term is well correlated with the increase of circulation observed in Figure 3.

Figure 6, which shows the 1263 m circulation tendencies at roughly twice the distance from the vortex, shows a much more transitory circulation evolution (note though from Tables 1 and 2 that the circulation at this distance is already very large and sufficient to account for the increases in circulation closer to the vortex when large scale convergence is present). There is also a lag in positive horizontal advection/stretching when compared

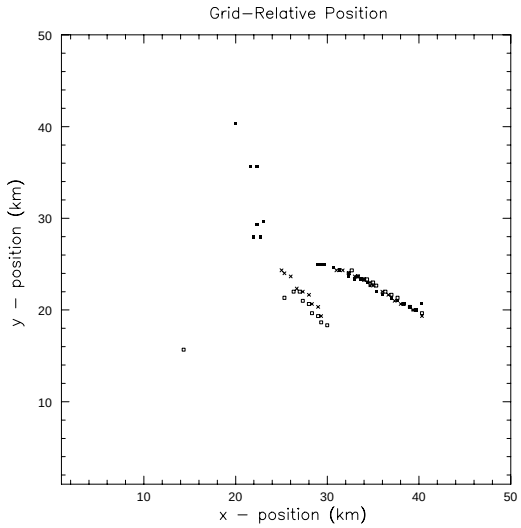

Figure 1: Grid position of maximum domain vertical vorticity, in 50 s increments after 2700 s. open squares – 19 m; crosses – 234 m; closed squares – 1263 m. Motion is to the east with time.

to vertical advection/tilting, and both are of the same order of magnitude.

6. CONCLUSION

The Eulerian method shows promise in providing a way to explain the behavior of numerically simulated vortices in a manner that is consistent with the numerical model. A larger number of circulation contours and a higher time density of analysis would be required, however, to provide the information that a trajectory analysis could provide.

7. ACKNOWLEDGMENTS

This study was funded by the National Science Foundation under grant ATM9900929.

8. REFERENCES

Adlerman, E.J., K.K. Droegemeier, and R. Davies-Jones, 1999: A numerical simulation of cyclic mesocyclogenesis. *J. Atmos. Sci.*, **56(13)**, 2045-2069.

Finley, C.A., 1997: Numerical simulation of intense multi-scale vortices generated by supercell thunderstorms. Ph.D. dissertation, Colorado State University, 297 pp.

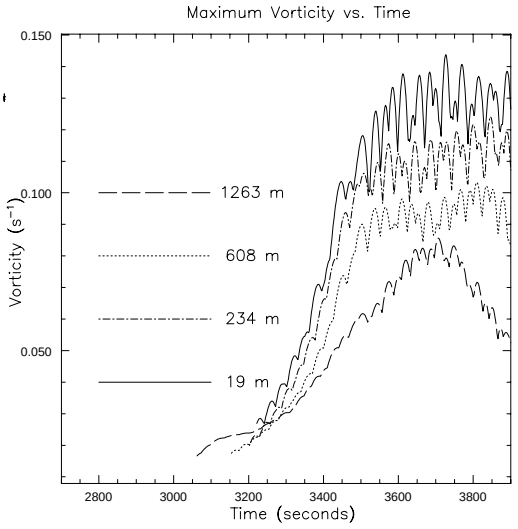

Figure 2: Maximum domain vertical vorticity vs. time. Plotted during period where vorticity centers follow the southeastward final track in Figure 1.

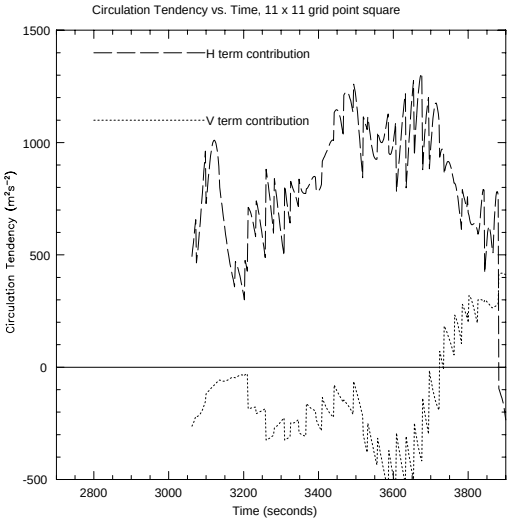

Figure 4: Circulation tendencies around square with side 11Δx centered at vorticity maximum, 1263 m above surface. H and V refer to the divergences of these terms in Equation 3. Plotted during period where vorticity center follows the southeastward final track in Figure 1.

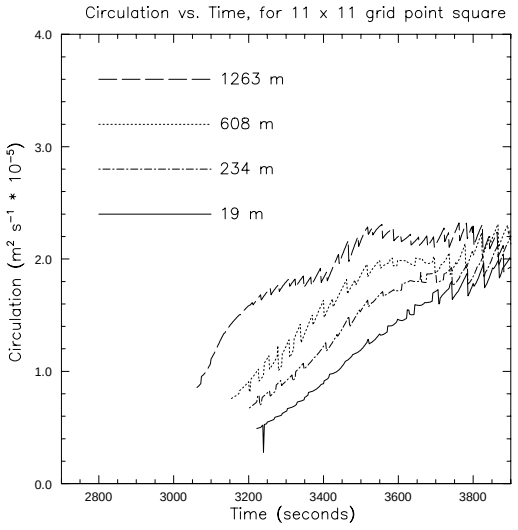

Figure 3: Circulation around square with side of 11 Δx, centered at vorticity maximum. Plotted during period where vorticity centers follow the southeastward final track in Figure 1.

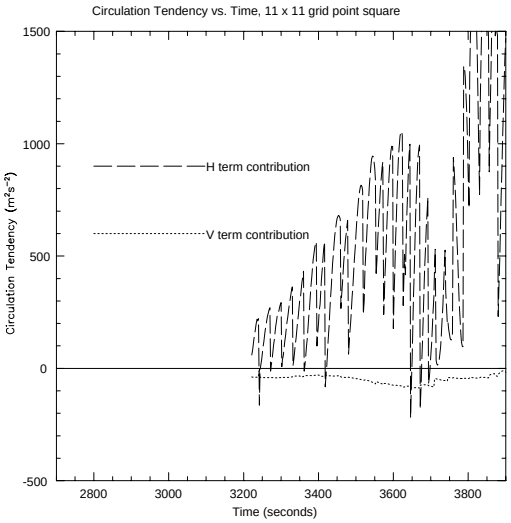

Figure 5: Same as Figure 4, but at 19 m above surface.

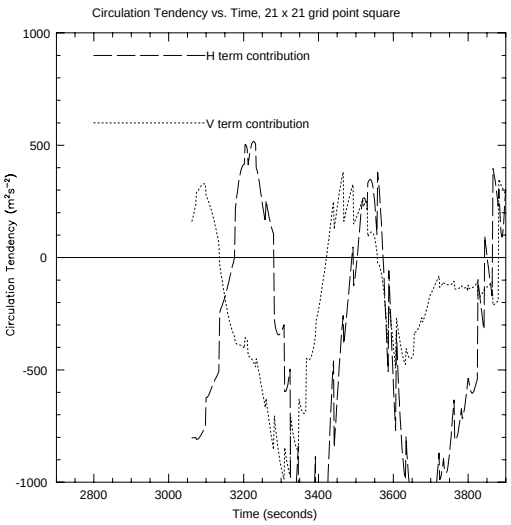

Figure 6: Same as Figure 4, but for square with side 21Δx.

19 m	234 m	608 m	1263 m	side length
4308	3923	3472	3292	1
23199	25122	25488	26992	3
33998	43562	51078	64275	5
48143	59476	74238	105444	7
58547	76329	96535	144120	9
63402	89339	118575	178439	11
71335	100088	142313	210267	13
77672	110429	166310	234263	15
80803	118727	188146	246301	17
84358	125749	208909	243876	19
86910	134093	227938	233777	21

Table 1: Circulation at 3300 s around square contours of various lengths centered about vorticity maxima, for 19 m, 234 m, 608 m, and 1263 m above surface. Units are m^2s^{-1} for circulation and Δx (333 m) for side length.

19 m	234 m	608 m	1263 m	side length
10857	11214	9139	7469	1
60763	61315	58714	49221	3
81590	93133	104618	96169	5
103979	128051	141914	141438	7
139510	158630	179150	184301	9
146463	170934	197435	217104	11
148148	183388	209003	243454	13
161348	193576	219855	271720	15
162336	194507	221488	298202	17
164827	196247	222648	316925	19
172496	196990	229295	325552	21

Table 2: Same as Table 1 but at 3600 s.

Grasso, L.D., 1996: Numerical simulation of the May 15 and April 26, 1991 tornadic thunderstorms. Ph.D. dissertation, Colorado State University, 151 pp.

Grasso, L.D., 2000: The dissipation of a left-moving cell in a severe storm environment. *Mon. Wea. Rev.*, **128**, 2797-2815.

Grasso, L.D., and W.R. Cotton, 1995: Numerical simulation of a tornado vortex. *J. Atmos. Sci.*, **52**, 1092-1203.

Haynes, P.H., and M.E. McIntyre, 1987: On the evolution of vorticity and potential vorticity in the presence of diabatic heating and frictional or other forces. *J. Atmos. Sci.*, **44(5)**, 828-841.

Klemp, J.B., and R. Rotunno, 1983: A study of the tornadic region within a supercell thunderstorm. *J. Atmos. Sci.*, **40**, 359-377.

Leslie, L.M., 1971: The development of concentrated vortices: A numerical study. *J. Fluid Mech.*, **48**, 1-21.

Pielke, R.A., W.R. Cotton, R.L. Walko, C.J. Tremback, M.E. Nicholls, M.D. Moran, D.A. Wesley, T.J. Lee, and J.H. Copeland, 1992: A comprehensive meteorological modeling system – RAMS. *Meteor. Atmos. Phys.*, **49**, 69-91.

Rotunno, R., and J.B. Klemp, 1985: On the rotation and propagation of numerically simulated supercell thunderstorms. *J. Atmos. Sci.*, **42**, 271-292.

Trapp, R.J., and R. Davies-Jones, 1997: Tornadogenesis with and without a dynamic pipe effect. *J. Atmos. Sci.*, **54**, 113-133.

Weisman, M.L. and C.A. Davis, 1998: Mechanisms for the generation of mesoscale vortices within quasi-linear convective systems. *J. Atmos. Sci.*, **55(16)**, 2603-2622.

Wicker, L.J., and R.B. Wilhelmson, 1995: Simulation and analysis of tornado development and decay within a three-dimensional supercell thunderstorm. *J. Atmos. Sci.*, **52**, 2675-2703.